

Characterization of Au/CdTe nanocomposites prepared by electrostatic interaction

Mohammad Mahbub RABBANI¹, Dae-geun NAM², Dae-han KIM³, Weontae OH³

1. Department of Bio-Fibers and Materials Science, Kyungpook National University, Daegu 702-701, Korea;

2. Dongnam Regional Division, Korea Institute of Industrial Technology, Busan 618-230, Korea;

3. Department of Materials and Components Engineering, Dong-Eui University, Busan 614-714, Korea

Received 2 May 2012; accepted 26 September 2012

Abstract: Au/CdTe nanocomposites were prepared by electrostatic interaction between oppositely-charged gold (Au) and cadmium telluride (CdTe) nanoparticles. Au and CdTe nanoparticles were stabilized by 4-(dimethylamino)pyridine (DMAP) and 3-mercaptopropionic acid to develop positive and negative charges on their surfaces in aqueous solutions, respectively. The red shifts of the surface plasmon absorptions with the increase of Au content indicate that the sizes of the nanocomposites expanded due to the complex formation. Mixing ratio of Au and CdTe nanoparticles controls the structure of the resulting composites effectively. Moreover, the sizes and shapes of the mixed nanoparticles are important parameters for the formation of metal/semiconductor nanocomposites. The Au/CdTe nanocomposites were characterized by small angle X-ray scattering technique (SAXS), transmission electron microscopy (TEM), cyclic voltammetry (CV) and X-ray photoelectron spectroscopy (XPS).

Key words: electrostatic interaction; gold nanoparticles; CdTe nanoparticles; nanocomposites

1 Introduction

Nanoparticles are always synthesized with different stabilizers or reducing agents to control their structures and to change their properties which are mainly dependent on their surfaces [1]. Thus, metal and semiconductor nanoparticles have been prepared with differently-charged stabilizers to develop positive or negative charges on their surfaces in aqueous solution. Surface modification of semiconductor nanoparticles provides some potential applications especially in light-emitting devices (LEDs) and biological labels [1–3]. Metal nanoparticles such as gold nanoparticles are considered stable in colloidal solutions, and they have also wide range of applications [1,4].

Recently, metal/semiconductor nanocomposites have attracted much interest to the scientists due to their characteristic optical, electronic and photonic properties [5–8], wide-ranging charge dynamics [9,10], and surface enhanced Raman scattering (SERS) effect [9,11]. Furthermore, they could be synthesized in order to obtain the specifically-tailored materials with improved

properties [10]. Because of the van der Waals interaction between heterogeneous species, some physicochemical properties such as enhancement of surface interaction, reactivity, selectivity etc can be modified [6,10].

Electrostatic assembly of oppositely-charged metal nanoparticles and semiconductor nanoparticles is an effective method to prepare metal-semiconductor nanocomposites [1,9,10,12]. The structures of these nanocomposites can be modified by adjusting the mixing ratios of the nanoparticles [9,10,12]. YANG et al [1] have investigated the electrostatic interaction between Au and CdTe nanoparticles and the optical properties of Au/CdTe nanocomposites, but their basic characteristics such as structures, binding characteristics, charge characteristics and electrochemical behavior are still remaining for further investigation.

In this study Au/CdTe nanocomposites were prepared by electrostatic interaction between positively-charged gold (Au) and negatively-charged cadmium telluride (CdTe) nanoparticles in aqueous solution. Structural analysis of the composites was carried out by small angle X-ray scattering technique (SAXS) and

transmission electron microscopy (TEM). Electrochemical behaviors were studied by cyclic voltammetry (CV). X-ray photoelectron spectroscopic (XPS) results were used to analyze the interaction between the heterogeneous nanoparticles and to investigate their binding characteristics. Optical properties were characterized by UV/Vis spectroscopy.

2 Experimental

All of the chemicals were used in as-received state without further purification. Sodium borohydride (NaBH_4 , 98%), hydrogen tetrachloro aurate trihydrate ($\text{HAuCl}_4 \cdot 3\text{H}_2\text{O}$), tetra-*n*-octylammonium bromide (TOAB), 4-(dimethylamino)pyridine (DMAP), tellurium powder (Te, 99.8%, <75 μm), 3-mercaptopropionic acid were purchased from Sigma-Aldrich, and anhydrous cadmium chloride (CdCl_2 , 99%) from Fluka. Water was distilled using a water distillation system (Dongwon Scientific., Ltd.).

Gold nanoparticles (GNPs) were synthesized following the method developed by BRUST et al [13]. To develop positive charges on the surfaces of GNPs, they were further modified with DMAP by a method described in Refs. [14,15]. Briefly, 30 mL (30 mmol/L) aqueous solution of $\text{HAuCl}_4 \cdot 3\text{H}_2\text{O}$ was reduced by 25 mL (0.4 mol/L) NaBH_4 aqueous solution in the presence of 80 mL (25 mmol/L) TOAB solution in toluene. After 30 min, the toluene phase was separated from the aqueous phase and it was washed with 0.1 mol/L H_2SO_4 , 0.1 mol/L NaOH, and distilled water, successively. Afterwards, GNPs in toluene were dried over anhydrous Na_2SO_4 . To obtain positively-charged GNPs, a certain amount of GNPs in toluene was added to the same volume of 0.1 mol/L DMAP aqueous solution. This process causes a spontaneous substitution of TOAB from GNP surfaces by DMAP and then DMAP-stabilized GNPs moved to the water phase.

Thiol capped cadmium telluride (CdTe) nanoparticles were synthesized in aqueous solution based on the method reported by ZHANG et al [16]. Briefly, 0.080 g (2.11 mmol) NaBH_4 , 0.128 g (1.00 mmol) tellurium powder and 1 mL distilled water were transferred to a small flask and quickly sealed with parafilm, which had a small pinhole to vent the gaseous byproducts. The reaction flask was placed in an ice bath and stirred for overnight. The resulting NaHTe was added to the CdCl_2 solution in the presence of stabilizer, 3-mercaptopropionic acid, under N_2 atmosphere. 3-mercaptopropionic acid stabilizes CdTe nanoparticles by the thiol group bounded to the surfaces of the particles, leaving the carboxylic acid group in water

medium. The molar ratio of Cd^{2+} /stabilizer/ HTe^- was fixed at 1:2.4:0.5. The resulting mixture was then refluxed for 10 h with stirring. pH of the reaction mixture was adjusted to ~9 by adding NaOH. The aqueous solution of CdTe nanoparticles was filtered out with a syringe filter with a pore size of 0.2 μm before use.

Finally, Au/CdTe nanocomposites were prepared by mixing different volume ratios of GNPs and CdTe nanoparticles. The mixing ratios of GNPs and CdTe nanoparticles were maintained as 1:20, 1:9, 1:5, and 1:0.2 (v/v), respectively. The Au/CdTe composites with excess amount of CdTe formed an optically transparent solutions but a comparable amount of the components resulted in precipitation. The mixture solution was agitated to prepare a homogeneous Au/CdTe composite mixture.

UV/Vis spectra were collected using a SCINCO-S3100 spectrophotometer in the range of 400–800 nm with water as blank. Transmission electron microscopy (TEM) images were obtained using JEOL 2100F microscope. TEM samples were prepared on 200-mesh copper grids by dip coating in dilute solutions. X-ray photoelectron spectroscopy (XPS) measurement of Au/CdTe nanocomposites was carried out by VG Scientific Escalab 250 at KBSI (Busan, Korea). All of the binding energies were determined with the C 1s core level peak at 284.6 eV as a reference. Cyclic voltammetry (CV) was carried out in a 0.5 mol/L H_2SO_4 aqueous solution by using an electrochemical workstation (SP-150 BioLogic Science Instruments) with a platinum gauze counter electrode, gold working electrode and a saturated calomel electrode (SCE) as reference electrode. A scan rate of 100 mV/s was used for the measurement and the applied voltage range was from 1.5 V to -1.0 V. Synchrotron small angle X-ray scattering (SAXS) experiments were performed at the bending magnet SAXS beamline 4 C1 of the Pohang light source in Korea [17,18]. SAXS patterns were recorded using a two-dimensional charge-coupled detector (2D CCD) (MAR165, USA). A light source from a bending magnet of the PLS storage ring was focused with a toroidal silicon mirror coated with platinum and monochromatized with a W/B4C double multiplayer monochromator, giving an X-ray beam of wavelength 1.45 Å. The scattering of solvent, water, was subtracted. Each solution was filtered using a syringe filter of pore size of 0.2 μm before measurement.

3 Results and discussion

Figure 1 shows the UV/Vis absorption spectra obtained from a series of Au/CdTe nanocomposites. The

characteristic surface plasmon bands of CdTe at 502.7 nm shifted towards a longer wavelength with increasing the amount of Au nanoparticles. This red shift of the composites was caused by the growth of particle sizes due to the composite formation [9,19]. A little broadening of the band shapes with the increase of Au contents might be caused by the weak electrostatic interfacial interaction between GNPs and CdTe nanoparticles [20]. The spectra were certainly obtained from the composites rather than the simple sum of both components [9]. During the preparation of Au/CdTe composites with various mixing ratios of GNPs and CdTe nanoparticles, it was found that an excess amount of CdTe in a small amount of GNPs made the mixture solution optically clear, but a mixture solution with similar amounts of GNPs and CdTe resulted in precipitation. In the former solution, the mixed GNPs and CdTe nanoparticles formed inorganic complex-like structures. The outer-shells covered with the equal-charged GNPs, resulting in a stable dispersion because of repulsive electrostatic interactions [12]. However, the equally-charged GNPs and CdTe nanoparticles in the other solution formed superlattice structures to precipitate easily [9,12].

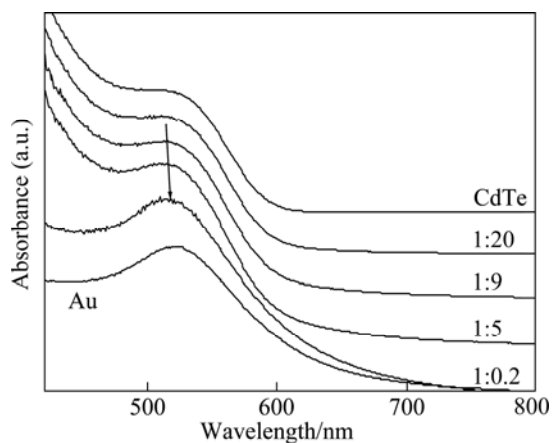


Fig. 1 UV/Vis absorption spectra of Au/CdTe composites with different Au contents (1:20 to 1:0.2 indicate the mixing ratios of Au to CdTe, respectively)

The nanostructures of the GNPs, CdTe nanoparticles and their Au/CdTe nanocomposites were deliberately investigated by transmission electron microscopy (TEM) and small angle X-ray scattering experiment. Figure 2 shows the TEM images of GNPs and CdTe nanoparticles. Unfortunately, we could not obtain any reliable image from Au/CdTe composites. From these images it can be found that both of the Au and CdTe nanoparticles are homogeneously distributed with similar sizes of ~ 3 nm. However, the CdTe

nanoparticles seem to be more agglomerative than Au nanoparticles. These TEM results were also supported by the absorbance of UV/Vis spectra shown in Fig. 1. The absorbance difference of Au and CdTe nanoparticles was limited only within a few nanometers.

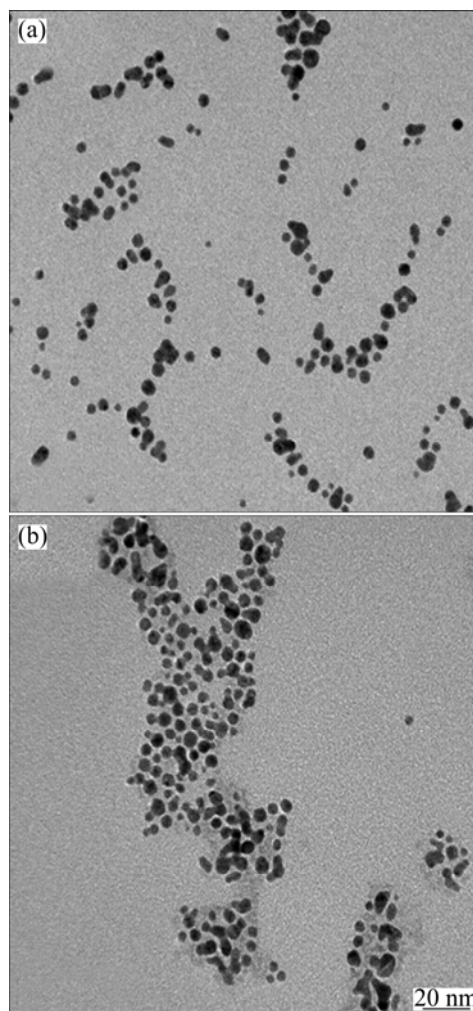


Fig. 2 TEM images of GNPs (a), and CdTe (b) nanoparticles

The reason for that we didn't find any TEM image from Au/CdTe nanocomposites is the uniformity of Au and CdTe nanoparticles in their sizes. When the counter-charged GNPs and CdTe nanoparticles are mixed together in a solution, it is expected that their complexed structures are formed and dispersed stably in the solution medium if the size of one species is much smaller than that of the counter-charged another, and the smaller one is excessively used for the composite preparation. Instead, it is difficult to expect the stable and complex-like composites from Au and CdTe nanoparticles of the similar sizes. The counter-charged and similar sized nanoparticles form the macrostructures easily by the iterated deposition of the counter-charged nanoparticles and finally precipitate in the mixture solution. Moreover,

CdTe nanoparticles are relatively unstable than Au nanoparticles. This result indicates that equally-sized and counter-charged nanoparticles are not favorable for the preparation of stable metal/ semiconductor nanoparticles, and hence their nanocomposites are immediately precipitated rather than remain dispersed in the solution for a long time.

Small angle X-ray scattering (SAXS) provides more information about the exact sizes and shapes of the nanoparticles dispersed in solutions [21]. Figure 3 shows the one dimensional (1D) SAXS profiles and Kratky plots. Figure 3(a) shows the SAXS profiles, which were obtained from Au, CdTe nanoparticles and their mixture solutions with different Au contents. The SAXS profile of CdTe nanoparticles linearly decreased with increasing q value in logarithm scale, whereas that of Au nanoparticles was plotted for the typical profile of globular shaped nanoparticles. The size of Au nanoparticles was estimated to be ~ 3.2 nm. However, CdTe nanoparticles were not monodisperse in the solution. These results agreed with the TEM images.

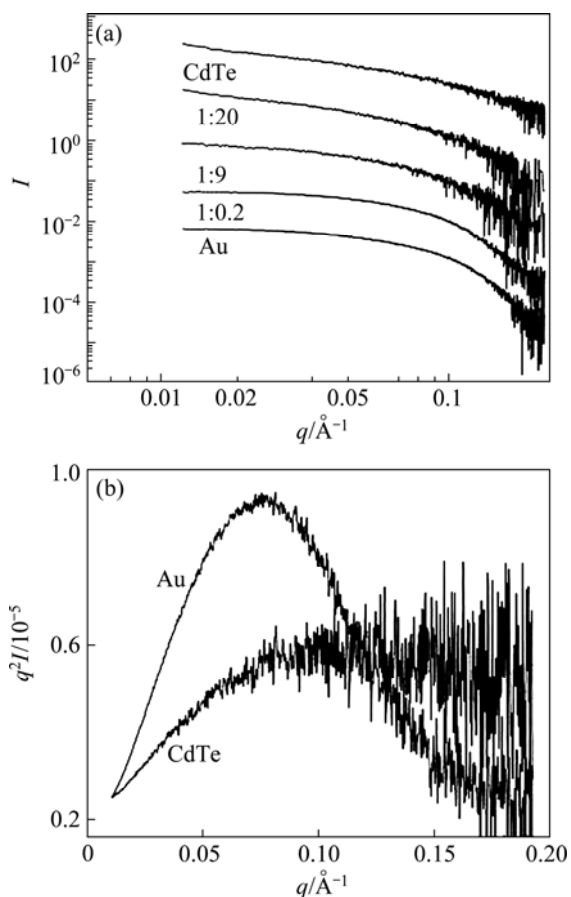


Fig. 3 SAXS profiles of GNPs, CdTe nanoparticles and their Au/CdTe composites: (a) Experimental SAXS profiles; (b) Kratky plot of GNPs and CdTe nanoparticles (The ratios in Fig.3 (a) indicate the volume ratios of Au/CdTe mixture solutions)

CdTe nanoparticles were relatively unstable and they agglomerated in solution. The entire SAXS profiles looked similar to the profile of CdTe nanoparticles with the increase of CdTe content in the mixture solution. The distinct structural difference of Au and CdTe nanoparticles could be compared from the Kratky plot of Fig. 3(b), which shows the globular shape but not the ideal spheres of Au nanoparticles. The Kratky plot of CdTe nanoparticles has no peak and is scattered with increasing q values, which indicates that the CdTe nanoparticles were unstable and their shapes and sizes were diverse in the solution.

Figure 4 shows the XPS results which were obtained from GNPs, CdTe nanoparticles and their Au/CdTe nanocomposites. The binding energies of elements and their shifts are important evidences to analyze the stoichiometry and binding characteristics of these elements in a given composite system. Depending on the interfacial environment, the binding energies of a given element can be shifted towards the higher or the lower position [22–24]. In addition, the binding energies of element adjacent to an oppositely-charged element are considerably dependent on the charge characteristics of the components [25]. These shifts of binding energies are caused by the redistribution of interfacial electrons due to the strong interaction between the neighboring elements [24]. The binding energies of Cd and Te in Au/CdTe composites were compared with those of pure CdTe nanoparticles in Figs. 4 (a) and (b). It was found from the XPS data that the binding energies of Cd and Te in Au/CdTe composites shifted towards the higher energies, Cd $3d_{3/2}$ 410.5 eV and Cd $3d_{5/2}$ 403.8 eV for CdTe nanoparticles, and 410.8 eV and 403.9 eV for Au/CdTe composite, Te $3d_{3/2}$ 579.7 eV and Te $3d_{5/2}$ 569.5 eV for CdTe nanoparticles, and 581.0 eV and 570.7 eV for Au/CdTe composite. These higher shifts of binding energies might be caused by the strong attraction between counter-charged GNPs and CdTe [26]. The strong attractive interaction could stabilize the CdTe nanoparticles binding together with GNPs, resulting in the surface electrons of CdTe nanoparticles shifting towards the higher binding energies [24]. Compared to binding energies of Au 4f peaks measured in GNPs, it is quite difficult to identify their shifts in Au/CdTe composite. Instead, the peaks broadened in the composite. Although there was no distinct change of binding energies, the peak broadening was due to the interfacial interaction between the adjacent elements.

The electrochemical behavior of the Au/CdTe nanocomposites was studied by cyclic voltammetric experiments shown in Fig. 5. The CV curves of Au/CdTe nanocomposites were compared with the CV curve

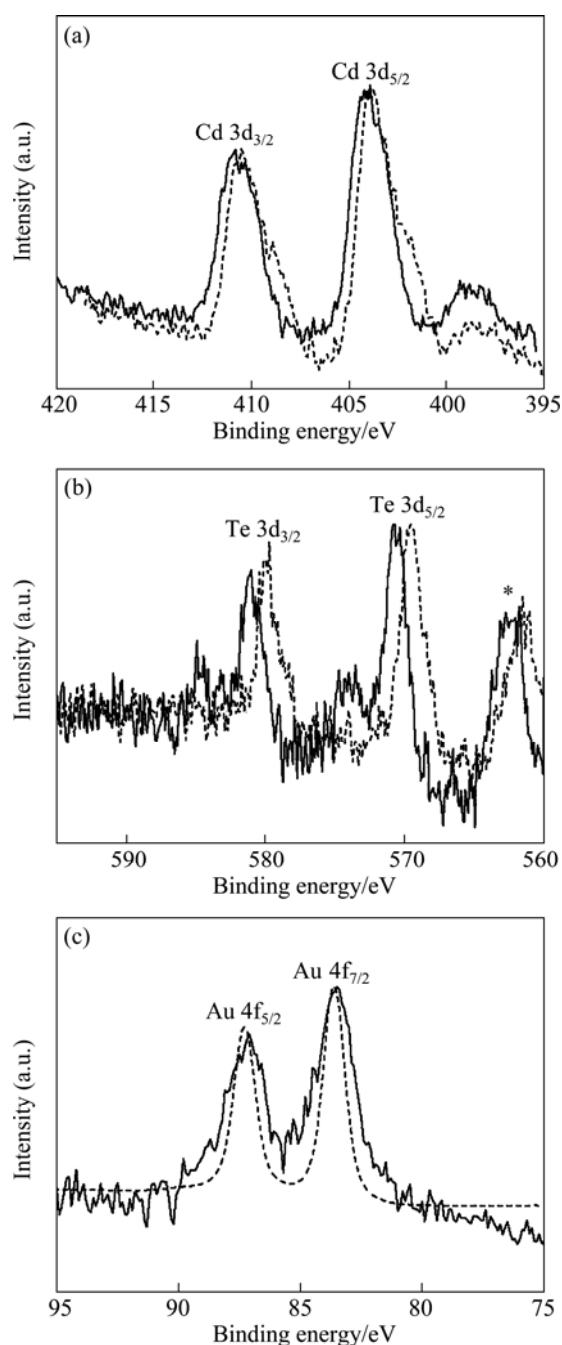


Fig. 4 XPS spectra obtained from Au/CdTe nanocomposites: (a) Cd 3d peaks of CdTe; (b) Te 3d peaks of CdTe; (c) Au 4f peaks of Au (Dot and solid lines represent element peaks, which were collected from pure state and their Au/CdTe (1:9) nanocomposites, respectively). The XPS spectra obtained from the other composites with different Au contents have the same pattern so they are not shown here. The asterisk (*) in Fig. 4(b) is ascribed to a ghost peak)

obtained from CdTe nanoparticles. Au/CdTe nanocomposites were oxidized at ~ 1.06 V and reduced at ~ 0.04 V in a cycle over the potential region measured.

The oxidation current was much higher than reduction current. The same phenomenon was observed for CdTe nanoparticles in our previous work [22]. The

redox peak positions of the composites with different Au contents did not shift remarkably but the current intensity was reduced with the increase of Au contents. This result indicates that Au content has very negligible contribution to the redox potential of CdTe in their composites but the electron transport has been little bit restricted with the increase of Au content due to the interfacial electron cloud redistribution caused by the electrostatic interaction between the oppositely charged nanoparticles.

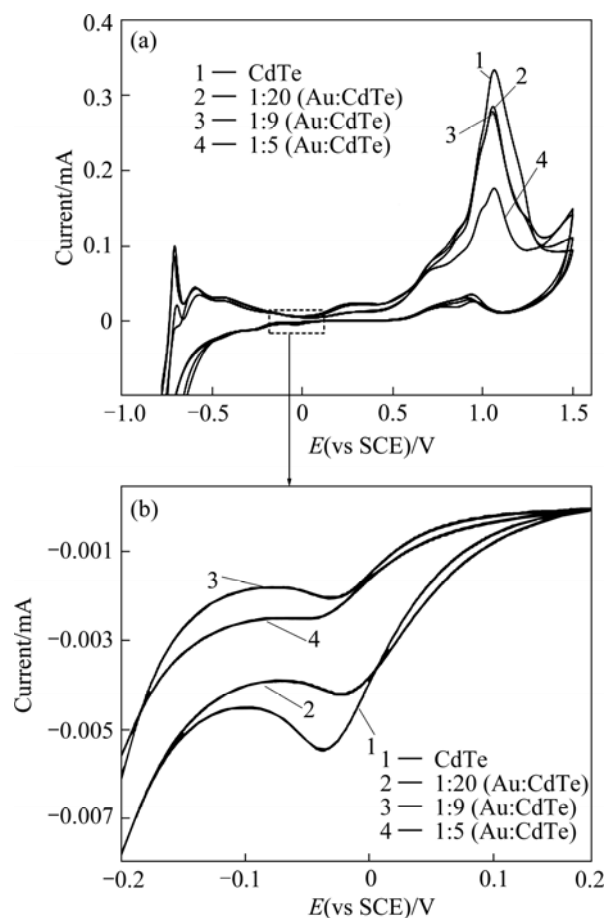


Fig. 5 Cyclic voltammograms obtained from CdTe nanoparticles, and their Au/CdTe nanocomposites with different Au contents (Fig. 5(b) is the enlargement. The measurements were conducted in a 0.5 mol/L H_2SO_4 solution at a scan rate of 100 mV/s and reference electrode was SCE)

4 Conclusions

1) Through the electrostatic interaction between oppositely-charged Au and CdTe nanoparticles, a series of Au/CdTe nanocomposites were prepared in aqueous solution.

2) The red shift of the surface plasmon absorptions of the nanocomposites indicates that the sizes of Au/CdTe nanocomposites increased with the increase of Au contents.

3) The actual image of Au/CdTe nanocomposite could not be identified from the TEM images. Instead, identical sizes of Au and CdTe nanoparticles were observed.

4) SAXS studies showed that Au and CdTe nanoparticles were globular- and irregular-shaped in solution states, respectively.

5) Cyclic voltammetry results indicated that GNPs hardly contributed to the change of redox potentials, but restricted the electron transport in their composites, which agreed with XPS results.

Acknowledgement

Authors thank to the support from LG Yonam Foundation.

References

[1] YANG D, WANG W, CHEN Q, HUANG Y, XU S. Electrostatic assembles and optical properties of Au–CdTe QDs and Ag/Au–CdTe QDs [J]. *Physica E*, 2008, 40(10): 3072–3077.

[2] GAO M, SUN J, DULKEITH E, GAPONIK N, LEMMER U, FELDMANN J. Lateral patterning of CdTe nanocrystal films by the electric field directed layer-by-layer assembly method [J]. *Langmuir*, 2002, 18(10): 4098–4102.

[3] WANG D, ROGACH A L, CARUSO F. Semiconductor quantum dot-labeled microsphere bioconjugates prepared by stepwise self-assembly [J]. *Nano Letters*, 2002, 2(8): 857–861.

[4] FELDHEIM D L, FOSS C A. *Metal nanoparticles: Synthesis, characterization and applications* [M]. New York: Dekker, 2000.

[5] YANG J, ELIM H I, ZHANG Q B, LEE J Y, JI W. Rational synthesis, self-assembly, and optical properties of PbS–Au heterogeneous nanostructures via preferential deposition [J]. *Journal of American Chemical Society*, 2006, 128(36): 11921–11926.

[6] MOKARI T, ROTHENBERG E, POPOV I, COSTI R, BANIN U. Selective growth of metal tips onto semiconductor quantum rods and tetrapods [J]. *Science*, 2004, 304(5678): 1787–1790.

[7] LEE J, GOVOROV A O, DULKA J, KOTOV N A. Bioconjugates of CdTe nanowires and Au nanoparticles: Plasmon-exciton interactions, luminescence enhancement, and collective effects [J]. *Nano Letters*, 2004, 4(12): 2323–2330.

[8] KAMAT P V. Photoinduced transformations in semiconductor–metal nanocomposite assemblies [J]. *Pure Applied Chemistry*, 2002, 74(9): 1693–1706.

[9] WANG Y, LI M, JIA H, SONG W, HAN X, ZHANG J, YANG B, XU W, ZHAO B. Optical properties of Ag/CdTe nanocomposite self-organized by electrostatic interaction [J]. *Spectrochimica Acta Part A*, 2006, 64(1): 101–105.

[10] KUMAR A, CHAUDHARY V. Optical and photophysical properties of Ag/CdS nanocomposites—An analysis of relaxation kinetics of the charge carriers [J]. *Journal of Photochemistry and Photobiology A*, 2007, 189(2–3): 272–279.

[11] ZOU S, WEAVER M J. Surface-enhanced Raman spectroscopy of cadmium sulfide/cadmium selenide superlattices formed on gold by electrochemical atomic-layer epitaxy [J]. *Chemical Physics Letters*, 1999, 312(2–4): 101–107.

[12] KOLNY J, KORNOWSKI A, WELLER H. Self-organization of cadmium sulfide and gold nanoparticles by electrostatic interaction [J]. *Nano Letters*, 2002, 2(4): 361–364.

[13] BRUST M, SCHIFFRIN D J, BETHELL D, KIELY C J. Novel gold-dithiol nano-networks with non-metallic electronic properties [J]. *Advanced Materials*, 1995, 7(9): 795–797.

[14] GITTINS D I, CARUSO F. Spontaneous phase transfer of nanoparticulate metals from organic to aqueous media [J]. *Angewandte Chemie International Edition*, 2001, 40(16): 3001–3004.

[15] RABBANI M M, KO C H, BAE J S, YEUM J H, KIM I S, OH W. Comparison of some gold/carbon nanotube composites prepared by control of electrostatic interaction [J]. *Colloids and Surfaces A*, 2009, 336(1–3): 183–186.

[16] ZHANG H, ZHOU Z, YANG B, GAO M. The influence of carboxyl groups on the photoluminescence of mercaptocarboxylic acid-stabilized CdTe nanoparticles [J]. *The Journal of Physical Chemistry B*, 2003, 107(1): 8–13.

[17] BOLZE J, KIM J, HUANG J Y, RAH S, YOUN H S, LEE B, SHIN T J, REE M. Current status of the synchrotron small-angle X-ray scattering station BL4C1 at the Pohang accelerator laboratory [J]. *Macromolecular Research*, 2002, 10(1): 2–12.

[18] YU C J, KIM J, KIM K W, KIM G H, LEE H S, REE M, KIM K J. Performance test of 4C1 beamline for protein solution scattering at the PLS [J]. *Journal of the Korean Vacuum Society*, 2005, 14(3): 138–142.

[19] ZHANG H, WANG L, XIONG H, HU L, YANG B, LI W. Hydrothermal synthesis for high-quality CdTe nanocrystals [J]. *Advanced Materials*, 2003, 15(20): 1712–1715.

[20] LINK S, EL-SAYED M A. Size and temperature dependence of the plasmon absorption of colloidal gold nanoparticles [J]. *The Journal of Physical Chemistry B*, 1999, 103(21): 4212–4217.

[21] LEE G W, JIN K S, KIM J, BAE J S, YEUM J H, REE M, OH W. Small angle X-ray scattering studies on structures of alkylthiol stabilized-silver nanoparticles in solution [J]. *Applied Physics A: Materials Science & Processing*, 2008, 91(4): 657–661.

[22] RABBANI M M, KIM D, KIM H C, KO C H, PARK Y D, OH W. Electrostatic interaction of multi-walled carbon nanotubes composites with CdTe and CdSe nanoparticles [J]. *Metals and Materials International*, 2011, 17(2): 227–231.

[23] SHARMA S N, SHARMA H, SINGH G, SHIVAPRASAD S M. Low energy ion induced effects on TOPO capped CdSe nanocrystals probed by XPS depth profiling and optical measurements [J]. *Nuclear Instruments and Methods in Physics Research Section B*, 2006, 244(1): 86–90.

[24] RABBANI M M, BAE J S, KIM D, KO C H, NAM D G, KIM Y, YEUM J H, OH W. Characterization of attractive interaction-driven carbon nanotube composites with Cd-Based nanoparticles [J]. *Journal of Nanoscience and Nanotechnology*, 2001, 11(7): 6453–6458.

[25] KIM J, RABBANI M M, KIM D, REE M, YEUM J H, KO C H, KIM Y, BAE J S, OH W. Structural and electrochemical properties of gold-deposited carbon nanotube composites [J]. *Current Applied Physics*, 2010, 10(2): s201–s205.

[26] COOPER T M, CAMPBELL A L, CRANE R L. Formation of polypeptide-dye multilayers by electrostatic self-assembly technique [J]. *Langmuir*, 1995, 11(7): 2713–2718.

Au/CdTe 纳米复合材料的静电作用制备及表征

Mohammad Mahbub RABBANI¹, Dae-geun NAM², Dae-han KIM³, Weontae OH³

1. Department of Bio-Fibers and Materials Science, Kyungpook National University, Daegu 702-701, Korea;
2. Dongnam Regional Division, Korea Institute of Industrial Technology, Busan 618-230, Korea;
3. Department of Materials and Components Engineering, Dong-Eui University, Busan 614-714, Korea

摘 要: 将相反电荷的纳米 Au 和纳米 CdTe 通过静电作用得到纳米复合 Au/CdTe 粒子。在水溶液中分别用二甲氨基吡啶和巯基丙酸稳定纳米 Au 和 CdTe 粒子, 使其表面分别带有正电荷与负电荷。Au/CdTe 纳米复合材料的表面等离子体吸收光谱随着 Au 含量的增加而红移, 表明纳米复合 Au/CdTe 粒子的长大是由于配位形成而引起的。纳米 Au 和纳米 CdTe 的比影响纳米复合 Au/CdTe 粒子的结构。复合纳米 Au/CdTe 粒子的尺寸和形状是影响金属/半导体纳米复合材料性能的重要参数。用小角 X 射线散射技术、透射电子显微镜、循环伏安法和 X 射线光电子能谱来表征纳米复合 Au/CdTe 粒子。

关键词: 静电作用; 纳米 Au; 纳米 CdTe; 纳米复合材料

(Edited by Hua YANG)